Metastable triplet state of the vacancy-oxygen center in silicon: An *ab initio* cluster study

A. B. van Oosten*
Huygens Laboratory, University of Leiden, P.O. Box 9504, 2300 RA Leiden, The Netherlands and Department of Physics and Measurement Technology, Linköping University, S-581 83 Linköping, Sweden

A. M. Frens and J. Schmidt
Huygens Laboratory, University of Leiden, P.O. Box 9504, 2300 RA Leiden, The Netherlands
(Received 23 February 1994)

An *ab initio* quantum chemical cluster study of the neutral vacancy-oxygen or $(V\text{-O})^0$ center in silicon, is presented, with emphasis on its metastable triplet state. We calculate a singlet-triplet splitting of 0.16 eV for $(V\text{-O})^0$. By calculation of the anisotropy of the nonradiative triplet life times we prove that the nonradiative decay occurs through combined spin-orbit and vibronic interaction. The observed C_{2v} off-center displacement is shown to be an effect of chemical bonding. Relaxation effects of nearest-neighbor Si and local vibrational modes are studied. As a check on the approach we study the effect of cluster size and compare our theoretical values for the hyperfine interactions with ^{17}O and the three nearest ^{29}Si neighbor shells to experiment.

I. INTRODUCTION

The vacancy-oxygen (V-O) center is the principal radiation defect produced in oxygen-rich crucible-grown silicon. It is one of the first and most thoroughly studied defects in silicon, and it is formed when interstitial oxygen captures a vacancy. (V-O) induces an acceptor level at E_c-0.17 eV and was first identified[1] by the electron paramagnetic resonance (EPR) of its negative charge state. Experimental evidence[2,3] exists for a donor level at E_c-0.76 eV. Besides a singlet ground state, which was studied by thermal reorientation[1] and by infrared absorption on a local mode,[4] $(V\text{-O})^0$ has a metastable triplet state[5,6] in the band gap. Because (V-O) exhibits a strong nonradiative recombination channel for free carriers, the center has attracted renewed interest. The recombination can be studied by observing the metastable triplet state with electron-spin echo (ESE) (Refs. 2 and 3) and optically detected magnetic-resonance (ODMR) (Ref. 7) techniques. A prominent feature of (V-O) is its off-center position along a [100] direction. C_{2v} symmetry was found experimentally for the singlet ground and the triplet metastable states of the neutral center as well as for the negatively charged center.[8] For the positive charge state we found C_{3v} symmetry. Spontaneous symmetry lowering is not unique to (V-O), but also occurs for substitutional nitrogen centers in silicon[9,10] and diamond,[11] which exhibit C_{3v} off-center behavior. There are indications that also the C(1s) core exciton in diamond[12] has symmetry lower than T_d.

In this paper we report an *ab initio* quantum chemical cluster study of $(V\text{-O})^0$ that was performed in support of an experimental investigation of electron recombination at this center. Its primary aims are to locate the energy position of the metastable triplet state with respect to the singlet ground state, and to establish the decay mechanism responsible for its strikingly anisotropic lifetime. More generally, the rich features of this experimentally very well-characterized center justify a complete theoretical characterization. At the same time (V-O) serves to test for the quantum chemical approach to defects and impurities in semiconductors.

In our treatment, many-electron wave functions are calculated with the *ab initio* Hartree-Fock-Roothaan (HFR) method. Important static correlation effects occur in the reconstructed bond of $(V\text{-O})^0$. Special attention is therefore paid to the variational balance in our description of the singlet and triplet states, so that a reliable value for the energy splitting is obtained. The spontaneous C_{2v} symmetry lowering bears no relation to the Jahn-Teller (JT) theorem, since in high symmetry there is no orbital degeneracy[13] in any of these cases. We show that the symmetry lowering is a chemical bonding effect. The anisotropy of the nonradiative triplet decay rates is estimated in a perturbation calculation of spin-orbit coupling effects. Ligand relaxation effects and the reorientation barrier are calculated. We confirm the identification of the observed 835-cm^{-1} (12-μ) infrared (IR) absorption with an antisymmetric ν_3 vibration. In an analysis of the hyperfine interactions, we show that many-electron or dynamic correlation effects are small for $(V\text{-O})^0$. They do, however, lead to observable hyperfine effects for $(V\text{-O})^-$.[8]

II. COMPUTATIONAL APPROACH

A. The quantum chemical hydrogen-terminated cluster approach

The natural approach to defects in semiconductors and ionic materials is based on a cluster model for the defect and its immediate surroundings. The disconnected bonds to the remaining crystal are terminated with hydrogen. For the calculation of the singlet-triplet splitting and also for the study of chemical bonding effects, the exact treatment of exchange is required. Therefore the electronic

structure is accurately computed by the *ab initio* methods of theoretical chemistry. Several defect calculations of this type have appeared in the literature,[14–17] but a study[18] of (V-O) was restricted to the negative charge state, while it employed pseudopotentials and small basis sets.

The calculations were done with the SYMOL package, which has the advantage over standard packages that in an open shell self-consistent-field (SCF) calculation the two-electron energy expression is completely user defined. This allows computation of wave functions with overlapping open shell orbitals to be computed within the Hartree-Fock-Roothaan formalism, as long as only Coulomb and exchange integrals appear in the two-electron energy. We use contracted Gaussian basis sets. For Si we adopt a $(12s8p \rightarrow 6s4p)$ split valence basis,[19] and for H a $(4s \rightarrow 1s)$ basis.[14] For oxygen a Huzinaga $(9s,5p)$ basis set was extended with a diffuse p function (exponent 0.11). The final $(9s,6p)$ basis set was contracted to $(3s,3p)$.[19,20]

The defect is modeled by a cluster typically consisting of the oxygen atom surrounded by 4–10 silicon neighbors. The bonds connecting the cluster to its crystal environment are saturated by hydrogen atoms. A Si-H bond length of 1.48 Å is used, which is the SCF optimum for Si_2H_6 and close to the experimental value. The Si-H bond length should not deviate significantly from the SCF optimum if the cluster model is to be relevant to crystalline silicon.[14] For geometry determinations we used the OSi_4H_{12} cluster (Fig. 1). At the optimum oxygen position we repeated the calculation on the larger $OSi_{10}H_{24}$ cluster (Fig. 1) in order to study the effect of the cluster size limitation.

B. The reconstructed bond

Consider two symmetry-equivalent orthogonal dangling-bond orbitals φ_1 and φ_2 localized at ligands Si_1 and Si_2 that are next-nearest neighbors. In the molecular-orbital (MO) approach, one would first form a bonding and antibonding combination

$$a_1=\frac{1}{\sqrt{2}}(\varphi_1+\varphi_2)\ ,\quad b_1=\frac{1}{\sqrt{2}}(\varphi_1-\varphi_2)\ , \tag{1}$$

and subsequently populate these with the appropriate number of electrons. The notation refers to the C_{2v} point group. Since a_1 has no nodal plane its orbital energy is lowest and the $^1A_1$ symmetric MO ground state would be

$$S_{\rm MO}=|a_1\bar{a}_1| =\tfrac{1}{2}(|\varphi_1\bar{\varphi}_1|+|\varphi_2\bar{\varphi}_2|+|\varphi_1\bar{\varphi}_2|-|\bar{\varphi}_1\varphi_2|)\ , \tag{2}$$

where all doubly occupied orbitals are suppressed in the notation for readability. In the actual calculations all electrons are included. In $S_{\rm MO}$ the electrons are completely uncorrelated. The first pair of determinants on the right-hand side describes an ionic wave function, corresponding to the symmetric combination of Si_1^--Si_2^+ and Si_1^+-Si_2^-. The second pair of determinants describes a covalent wave function corresponding to Si_1^0-Si_2^0, with strongly correlated electrons. The ionization potential of atomic Si is IP=8.149 eV, and the electron affinity is $A=1.385$ eV. Taking into account the Coulomb energy, the attraction of a ion pair of opposite charge, $V=3.750$ eV, we find the energy of the next-nearest-neighbor Si^+-Si^- pair to exceed that of a Si^0-Si^0 pair by IP-A-V=3.0 eV. Therefore the covalent wave function for the $^1A_1$ ground state,

$$S_0=\frac{1}{\sqrt{2}}(|\varphi_1\bar{\varphi}_2|-|\bar{\varphi}_1\varphi_2|)=\frac{1}{\sqrt{2}}(|a_1\bar{a}_1|-|b_1\bar{b}_2|)\ , \tag{3}$$

where dangling-bond orbitals are taken to be orthogonal, should be lower in energy by 1.5 eV. One can obtain this wave function by first forming Slater determinants from low-symmetry dangling bonds and then combining these into symmetry combinations. The symmetry is exhibited only at the many-electron level and not at the one-electron level, as in the MO approach. The triplet partner of S_0 has $^3B_1$ symmetry, and can be written

$$T_0=|\varphi_1\varphi_2|=|a_1b_1|=T_{\rm MO}(^3B_1)\ . \tag{4}$$

Here the dangling bond and the MO procedure give identical results because of Pauli correlation. Yet as the singlet version of T_0 the $^1B_1$ symmetric singlet MO theory would suggest

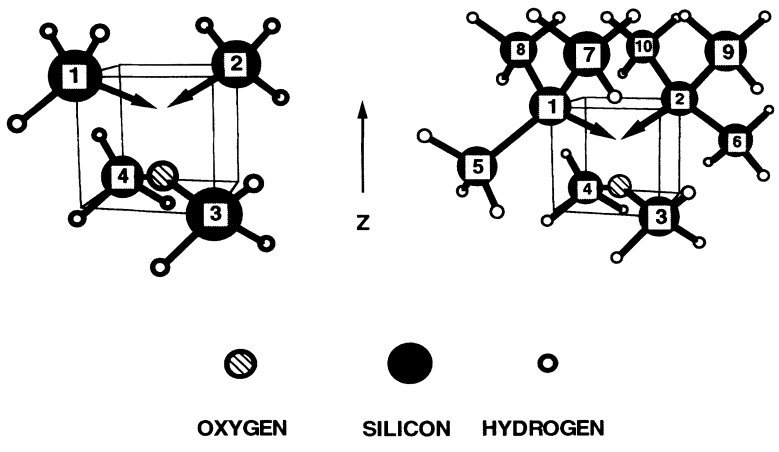

FIG. 1. The cluster models OSi_4H_{12} and $OSi_{10}H_{24}$.

$$S'_{\mathrm{MO}}=\frac{1}{\sqrt{2}}(|a_1\bar{b}_1|-|\bar{b}_1a_1|)=\frac{1}{\sqrt{2}}(|\varphi_1\bar{\varphi}_1|-|\varphi_2\bar{\varphi}_2|)\,, \tag{5}$$

which is ionic and should be 3 eV higher in energy.

If the orbitals in (3) and (4) were the same, S_0 would have a slightly higher energy than T_0 due to the positive direct exchange interaction

$$2K_{12}=\int \varphi_1(r_1)\varphi_2(r_1)\frac{1}{|r_1-r_2|}\varphi_1(r_2)\varphi_2(r_2)\,. \tag{6}$$

However, in the singlet the orbitals φ_1 and φ_2 are not restricted to be spatially orthogonal, as in the triplet state. Due to its additional variational freedom the singlet winds up below T_0. The nonorthogonal orbitals can be written

$$\varphi'_1=\frac{\varphi_1+p\varphi_2}{\sqrt{1+p^2}}\,,\quad \varphi'_2=\frac{\varphi_2+p\varphi_1}{\sqrt{1+p^2}}\,, \tag{7}$$

where the overlap is $S=2p/\sqrt{1+p^2}$. The fully relaxed singlet wave function becomes

$$S_0=\frac{1}{\sqrt{2}}(|\varphi'_1\bar{\varphi}'_2|-|\bar{\varphi}'_1\varphi'_2|)=\alpha|a_1\bar{a}_1|-\beta|b_1\bar{b}_1|\,, \tag{8}$$

with

$$\alpha^2=1-\beta^2=\frac{(1+p)^2}{(1+p)^4+(1-p)^4}\,. \tag{9}$$

This is the simplest case of a generalized valence bond[21] (GVB) wave function . The overlap S can be expressed in α and β as

$$S=\frac{\alpha-\beta}{\alpha+\beta}\,. \tag{10}$$

S is now treated as an extra variational parameter. The initial gain in one-electron energy—potential minus kinetic energy—is a first-order function, while the cost in two-electron energy—electron repulsion—energy is a second-order function of the overlap S. Therefore an energy minimum always results in nonzero S. Electron repulsion prevents the wave function from completely transforming into the MO form (2), and the remaining correlation in (8) could be termed the Coulomb correlation, to distinguish it from the stronger Pauli correlation.

The large correlation error of the MO singlet wave function reverses the order of the states, but the one-electron properties are much less affected. Consider the expectation value of a one-electron operator O taken to be diagonal in spin for simplicity. For the two-electron states discussed above, one finds that $\langle O\rangle$ has the form

$$\begin{aligned}\langle O\rangle&=2\alpha^2\langle a|O|a\rangle+2\beta^2\langle b|O|b\rangle\\&=\langle\varphi_1|O|\varphi_1\rangle+\langle\varphi_2|O|\varphi_2\rangle+\lambda\,\mathrm{Re}\langle\varphi_1|O|\varphi_2\rangle\,,\end{aligned} \tag{11}$$

where λ takes the values 2, 0, 0, and $2(\alpha^2\text{-}\beta^2)$, for states (2), (4), (5), and (8), respectively. Since $\langle\varphi_1|O|\varphi_2\rangle$ is small or zero for orbitals well localized on different sites, these four wave functions give practically the same result if orbital relaxation effects are unimportant. This explains why a MO approach can account for one-electron properties such as local mode frequencies.

C. Hyperfine interactions

Hyperfine interactions can provide valuable, unambiguous clues to the electronic structure and chemical constitution of defects. Extensive hyperfine data is available for $(V\text{-O})^0$. The detailed interpretation of these data is a prime objective of this work.

Hyperfine interactions are determined by the properties of the unpaired electrons in the vicinity of the nucleus, where the employed basis sets do not describe the wave function accurately. This is of no consequence for the chemical properties, so that an enlargement of the basis sets would increase the computational and integral storage effort greatly without improving the overall accuracy of the results. The calculation of hyperfine interactions can be simplified greatly by using the facts that the hyperfine Hamiltonian is to a very good approximation site diagonal, and that in the core region the radial dependence of the orbital is expected to be purely atomic, apart from a scaling factor. Therefore, in the vicinity of the nucleus we can write the valence orbitals as a linear combination of atomic orbitals. For the present case of s- and p-type valence orbitals we take

$$\varphi=c_s\varphi_s+c_x\varphi_x+c_y\varphi_y+c_z\varphi_z\,. \tag{12}$$

We estimate the scaling factors c_s and c_i $(i=x,y,z)$ from the ratio of the coefficients of the most localized basis function in the cluster and in the isolated atom. The basis set errors in the isolated atom and in the cluster should then to a large degree cancel out. The actual hyperfine interactions are obtained by scaling of atomic hyperfine interactions, for which accurate theoretical values exist. An unpaired electron in an orbital of the form (12) causes an axially symmetric magnetic hyperfine interaction that can be given in the well-known tensor form

$$A_{ij}=c_s^2A_s\delta_{ij}+A_p(3c_ic_j-c^2\delta_{ij})\,, \tag{13}$$

where the (i,j,k) takes values (x,y,z). The atomic Fermi contact interaction due to an s orbital φ_s is

$$A_s=\tfrac{2}{3}\mu_0\mu_B\mu_Ng_eg_n|\varphi_s(0)|^2\,. \tag{14a}$$

The atomic magnetic dipole interaction due to a p orbital is

$$A_b=\frac{1}{10\pi}\mu_0\mu_B\mu_Ng_eg_n\langle\varphi_p|r^{-3}|\varphi_p\rangle\,. \tag{14b}$$

The magnetic hyperfine interaction contains information about the spin localization $\eta^2=c_s^2+\Sigma c_i^2$ and the hybrid character and orientation c_i/η of the paramagnetic orbitals. The contributions of all partially occupied orbitals are to be summed.

A review of values for A_s and A_p for ^{17}O and ^{29}Si is given in Table I. Where available we have used Fraga's HF values,[22] which may differ by up to 30% from the more commonly used Hartree-Fock-Slater (HFS) results of Morton and Preston.[3] Fraga's values are more accu-

TABLE I. Atomic hyperfine parameters for silicon (^{29}Si) and oxygen (^{17}O). (a) Hartree-Fock-Slater (Ref. 23); (b) Hartree-Fock (Ref. 6); (c) Hartree-Fock (Ref. 22); and (d) experiment (Ref. 33).

	^{29}Si	^{17}O	Unit
$\|\varphi(0)\|^2$	34.52[a]	51.60[b]	Å^{-3}
$\langle r^{-3}\rangle^a$	18.16	39.275	Å^{-3}
$\langle r^{-3}\rangle^c$	13.862	33.566	Å^{-3}
$\langle r^{-3}\rangle^d$		33±2	Å^{-3}
A_s	−4542	−4633	MHz
A_p	−87.1	−143.9	MHz

rate since the HF method does not involve the local-density approximation. This is confirmed in the single case where an empirical value is available.

III. RESULTS

A. Oxygen off-center displacement

We calculated the three wave functions described in Sec. II: the MO singlet S_{MO}, the covalent singlet S_0, and the triplet T_0. We varied the oxygen position (00z) along the z axis from the T_d(000) to the D_{2d}(001) positions, with the remaining cluster atoms fixed. The resulting total cluster energies are displayed as a function of z in Fig. 2. At $z=0$ it is necessary to include all four dangling-bond orbitals in the wave function for S_0. Therefore (8) is replaced by

$$S_0=\frac{1}{2\sqrt{3}}\sum_{j>i}(|\varphi_i'\bar{\varphi}_j'|-|\bar{\varphi}_i'\varphi_j'|)$$
$$=\alpha|a_1\bar{a}_1|-\beta(|t_{2x}\bar{t}_{2x}|+|t_{2y}\bar{t}_{2y}|+|t_{2z}\bar{t}_{2z}|)\,, \quad (15)$$

where as before all doubly occupied orbitals are suppressed in the notation. The indices i and j run over the four dangling-bond sites. The orbitals a_1 and t_{2i} are T_d-symmetric linear combinations of dangling bonds on these sites. A similar form was used for small nonvanishing z, but now the t_2 determinants are replaced with C_{2v} ones based on a_1, b_1, and b_2 orbitals, each with a different coefficient. Figure 2 shows that the orbital singlets S_0 and S_{MO} have negative second derivatives at vanishing z, while the orbital triplet state T_0 has a negative first derivative at $z=0$. The possibility of a nonvanishing derivative for this case is indicated the Jahn-Teller theorem. In spite of this distinction all three states obtain their minimum energy for the same value of the oxygen off-center displacement $z=0.95$ Å. Moreover, a substantial change in the electronic structure takes place upon symmetry lowering. Clearly Jahn-Teller-type considerations are not relevant here, since these are based on symmetry considerations and small nuclear potential changes. The chemical bonding explanation of the off-center displacement is straightforward: oxygen is divalent, as in H_2O, and therefore saturates two out of four ligand dangling bonds. This interpretation finds support in the existence of the Si:HVH (Ref. 24) defect with similar properties, where the role of oxygen is played by hydrogen atoms.

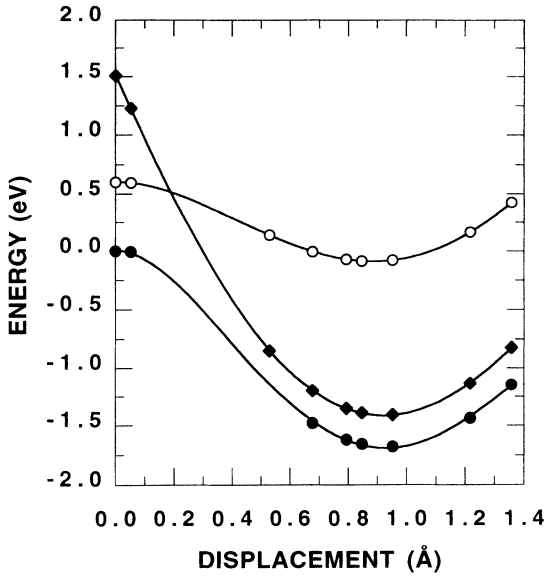

FIG. 2. Total energy of $[OSi_4H_{12}]^0$ vs C_{2v} oxygen displacement along z. ○: S_{MO}; ●: S_0; ♦: T_0.

The energy gain of S_0 in going from $z=0$ to the optimum position is 1.6 eV, while for S_{MO} the gain is only 0.6 eV. The difference is mainly due to an excessive increase in electron repulsion energy of 0.75 eV in S_{MO}, as can be seen from an atomic estimate similar to that in Sec. II. For T_0 the stabilization is 3 eV. The T_0 and S_0 curves are nearly parallel for z values away from $z=0$, with a distance of 266 meV at the optimum geometry. The overlap for optimum geometry was only $S=0.27$, which indicates that to a considerable degree each electron occupies its own dangling orbital. We repeated the calculation on $OSi_{10}H_{24}$, a cluster obtained from OSi_4H_{12} by replacing the six hydrogen atoms bonded to the dangling-bond atoms by six SiH_3 units. The singlet-triplet splitting was found to be 225 meV for this larger cluster. In Sec. III C we will see that the wave function of $OSi_{10}H_{24}$ corresponds to a localization of 90%. The reduction of the splitting by 18% with respect to its value in OSi_4H_{12} shows that it varies as the square of the localization on the dangling-bond atoms. On this ground we finally estimate the splitting will be 0.16 eV for the experimental value of the localization of 75%. The localization issue will be discussed in more detail in Sec. III C.

B. Lattice relaxation

Next we determined the effect of relaxation of Si_3 and Si_4, the neighbors involved in the Si-O bonds. These atoms were allowed to symmetrically move in the [1$\bar{1}$0] plane, while keeping the other atoms fixed. Minimal energy was reached for a large inward displacement of each atom along the [110] direction of 0.21 Å, giving an energy gain of 0.82 eV.

Relaxation effects at the dangling bond atoms $Si_{1,2}$ were found to be small: the unperturbed lattice position

was very close to optimal for the ground-state singlet S_0. For the triplet T_0 the optimal energy was reached for an outward displacement along $[1\bar{1}0]$ of only 0.03 Å. We reported similar small lattice relaxation effects at dangling orbital sites in a previous study[25] of the neutral vacancy. The result is physically plausible since in the perfect crystal equilibrium is reached when neighboring atoms exert a vanishing force upon one another. Removing an atom therefore should not result in a significant net force on its neighbors. Relaxation of its two neighbors did not alter the optimal position of oxygen. The optimal geometry was very closely the same for S_0 and T_0, and the change in singlet-triplet splitting as a result of geometry optimization was insignificant.

C. Hyperfine interactions

An important clue to the structure of $(V\text{-O})^0$ is constituted by the hyperfine interactions of the paramagnetic state T_0. The hyperfine interaction with the ^{17}O nucleus observed[6] in EPR is direct evidence of the presence of a single oxygen atom in the defect. Moreover the largest ^{29}Si hyperfine is resolved in EPR; the dominant spin localization on the next-nearest-neighbor pair $Si_{1,2}$ proves the dangling-bond character of the paramagnetic orbitals. The comparison of these hyperfine data with our theoretical values forms a stringent test on our wave functions and on the cluster approximation. Our theoretical values for the hyperfine interactions at the oxygen and silicon sites in the cluster $[OSi_4H_{12}]^0$ in the triplet state T_0 are displayed in column (a) of Table II and should be compared to the observed values in column (d). The ^{17}O hyperfine interaction is close to the experimental value, with the contact interaction too small by a factor of 0.6. Our values for the anisotropic hyperfine interaction at the mirror plane ligands Si_1 and Si_2 agree well with experiment, but are scaled up by 25% with respect to the experimental values. Delocalization is not accounted for in this small cluster. The contact interaction is overestimated by a factor of 2, which results in 25% s character. This is most likely due to our approximation of the contact interaction, since Mulliken population analysis gives 15% s character, close to the observed value of 12%. The influence of admixture of the lowest excited SCF state was calculated in the nonorthogonal configuration (NOCI) approach, of which the details will be given elsewhere.[8] This state has one electron excited from the reconstructed bond to the oxygen atom and its two silicon neighbors. The two-configuration results figure in column (b) of Table II. The effect is seen to be small.

The effect of cluster size was studied by comparing with $[OSi_{10}H_{24}]^0$. The results are listed in column (c) of Table II. The resulting interactions at O and $Si_{1,2}$ show a decrease of about 10% with respect to those of $[OSi_4H_{12}]^0$, which indicates that the absence of delocalization in $[OSi_4H_{12}]^0$ is a consequence of the cluster size limitation and not of the single determinant approximation. The larger cluster also allows calculation of the interaction with more distant ligand shells of mirror plane ($Si_{5,6}$) and low symmetry (Si_{7-10}). Experimentally, a partly resolved hyperfine interaction is observed for $B\|[111]$ with a relative intensity corresponding to a low-symmetry ligand shell. A published recorder trace[5] suggests that the second largest hyperfine occurs at a low-symmetry shell, consisting of four silicon ligands, with approximate [111]-axial symmetry and approximate main values of $A_\parallel = 21$ MHz and $A_\perp = 15$ MHz. Our theoretical prediction agrees with these data, as we find $A_\parallel = 15.3$ MHz and $A_\perp = 11.7$ MHz for the Si_{7-10} shell and smaller values, $A_\parallel = 12.6$ MHz, and $A_\perp = 8.7$ MHz, for the $Si_{5,6}$ shell. Moreover, both interactions have nearly [111]-axial symmetry. The predicted Si_{7-10} interaction is about 75% of the observed value, which is consistent with the slight overestimate of the localization on $Si_{3,4}$.

TABLE II. ^{17}O and near-neighbor ^{29}Si hyperfine interactions of $(V\text{-O})^0$ as obtained from the cluster $[OSi_4H_{12}]^0$: (a) $[OSi_4H_{12}]^0$, one configuration; (b) $[OSi_4H_{12}]^0$, two configurations; (c) $[OSi_{10}H_{24}]^0$, one configuration; and (d) experiment (Refs. 5 and 6).

Nucleus		a	b	c	d
O	A_s	−64.7	−73.4	−65.6	−113.1
	$A_{x'x'}$	9.8	9.6	9.3	9.6
	$A_{y'y'}$	−1.7	−1.9	−1.3	−3
	$A_{z'z'}$	−8.0	−7.5	−8.1	−6.6
$Si_{1,2}$	A_s	−353.2	−351.0	−306.9	−153.6
	A_{xx}, A_{yy}	0.2	0.2	0.6	0.0
	A_{zz}	−0.4	−0.4	−1.2	0.0
	A_{xy}	38.9	38.7	−35.9	30.3
	$A_{yz}, -A_{zx}$	39.1	39.0	−36.8	31.6
$Si_{5,6}$	$B\|(111)$			−12.6	
	$B_\perp(111)$			−9.7	
Si_{7-10}	$B\|(111)$			−15.3	
	$B_\perp(111)$			−11.7	

D. Triplet nonradiative decay

When electrons are excited from either the valence band, the C-line defect or from $(V\text{-O})^0$, their subsequent recombination results in $(V\text{-O})^-$ and $(V\text{-O})^0$. In the latter case some centers end up in the T_0-excited state and can be observed by magnetic resonance. The T_0 state is split by spin-spin interaction. The zero-field energies, relaxation rates, and symmetry properties are given in Table III. The three triplet sublevels are observed to decay at strikingly different rates. In the present section

TABLE III. Theoretical and experimental triplet sublevel decay rates of $(V\text{-O})^0$. Experimental values taken from Ref. 28.

Substate	Symmetry	Wave function	Decay rate (GHz)	
			experiment	this work
T_{0x}	$A_2 = B_1 \otimes b_2$	$\frac{i}{\sqrt{2}}\{\|12\| - \|\bar{1}\bar{2}\|\}$	0.50(3)	0.25
T_{0y}	$A_1 = B_1 \otimes b_1$	$\frac{1}{\sqrt{2}}\{\|12\| + \|\bar{1}\bar{2}\|\}$	4.7(3)	4.85
T_{0z}	$B_2 = B_1 \otimes a_2$	$\frac{1}{\sqrt{2}}\{\|1\bar{2}\| + \|\bar{1}2\|\}$	1.70(0.15)	1.35

we produce theoretical estimates for the relative decay rates.

The decay $T_0 \rightarrow S_0$ is possible because spin-orbit coupling (SOC) admixes excited triplet states T_n into the ground-state singlet S_0, and excited singlet states S_n into the lowest triplet state T_0. In this way, the nonradiative transition rate is[26] "stolen" from the transitions $S_n \rightarrow S_0$ and $T_n \rightarrow T_0$. According to first-order perturbation theory the wave functions for the lowest triplet state and the singlet ground state become

$$\underline{S}_0 = S_0 + \Sigma_i \frac{\langle T_i | H_{\text{soc}} | S_0 \rangle}{E_{T_i} - E_{S_0}} ,$$
$$\underline{T}_0 = T_0 + \Sigma_i \frac{\langle S_i | H_{\text{soc}} | T_0 \rangle}{E_{S_i} - E_{T_0}} . \tag{16}$$

The radiationless transition probabilities between $\underline{T}_0$ and $\underline{S}_0$ are governed by the matrix element $J = \langle \underline{S}_0 | H_{\text{vib}} | \underline{T}_0 \rangle$, where H_{vib} stands for the vibronic interaction. The corresponding matrix elements are

$$J_1 = \frac{\langle T_0 | H_{\text{vib}} | T_i \rangle \langle T_i | H_{\text{soc}} | S_0 \rangle}{E_{T_i} - E_{S_0}} ,$$
$$J_2 = \frac{\langle T_0 | H_{\text{soc}} | S_i \rangle \langle S_i | H_{\text{vib}} | S_0 \rangle}{E_{S_i} - E_{T_0}} . \tag{17}$$

Since SOC only has nonvanishing matrix elements between states of the same total symmetry, a specific state S_i is mixed with one of the three sublevels of T_0, and vice versa. Further, since E_{T_i}-E_{S_0} is not very different from E_{S_i}-E_{T_0}, we have to consider both terms J_1 and J_2. These two terms are of the same order of magnitude and have opposite signs since the SOC matrix elements are imaginary. As a consequence the nonradiative transition probability per unit time for the sublevel T_{0i} $(i = x,y,z)$ calculated according to the model of Robinson and Frosch[27] are given by

$$K_i = \frac{2\pi\rho}{\hbar} F (J_{1i} + J_{2i})^2 .$$

Here F represents the Franck-Condon factor and ρ the density of final states. We assume that these quantities are the same for all T_0 substates. Further, we assume that the vibronic parts in J_1 and J_2 are also equal. This means that the ratios of K_i are determined by the SOC matrix elements in (17). The excited states are effective-mass states, situated at the conduction-band edge, and cannot be computed with our cluster model. Now consider the valence electronic structure of the crystal surrounding the defect as consisting of doubly occupied sp^3 bonds. Each effective-mass state can then be decomposed into a linear combination of localized virtuals that result from the ground state (S_0 or T_0) by exciting an electron from the defect dangling-bond pair to a particular bond k. Thus for the singlet (triplet) effective-mass states one has

$$S_i = \Sigma_k C_{ik} \Psi_k^S , \tag{18}$$

and an analogous expression for the triplet states T_i. We assume that the expansion coefficients are the same for singlets and triplets. The index k is to be summed over all bonds excluding the two dangling bonds central to the defect. The radial SOC integrals are heavily weighed near the nucleus, so that only intra-atomic SOC matrix elements survive. Thus we only have to consider SOC with those virtuals in which the excited electron goes to one of the six backbonds of the dangling-bond atoms, to be referred to as $S(T)_1$. These virtual states can be computed in the cluster model. We assume that $\Sigma_n C_{nk}^2$ is equal for the six backbonds involved, so that this quantity does not influence the relative value of the decay rates. The orbital matrix elements in Eq. (17), like the hyperfine interactions, are largely determined by the core regions of the atoms involved. For their calculation we therefore follow the same method as in Sec. II for the anisotropic hyperfine interaction. Of the six virtuals involved, two have an electron moved to the backbonds 1–5 and 2–6, and can be combined in states of A_1 and B_1 orbital symmetries. The remaining four, to the backbonds 1–7, 1–8, 2–9, and 2–10, result in states with A_1, A_2, B_1, and B_2 orbital symmetries. The singlet $S_1(A_2)$, $S_1(B_1)$, and $S_1(B_2)$ states couple with T_{0z}, T_{0y}, and T_{0x}, respectively. Of the corresponding triplet states only substates with total A_1 symmetry couple with S_0, that is $T_{1z}(A_2)$, $T_{1y}(B_1)$, and $T_{1x}(B_2)$. The resulting theoretical decay rates are compared to the experimental values[28] in Table III. Considering the degree of approximation, the agreement with experiment is very satisfactory. Our result therefore gives theoretical support to the view that the triplet decay occurs through spin-orbit coupling.

E. Local vibrational modes

Since oxygen is lighter than silicon, local vibrational modes are observed in infrared (IR) absorption. The various possible modes are displayed in Fig. 3. $(V\text{-}O)^0$ in its singlet ground state gives rise to an IR absorption[4,29] with a low-temperature wave number of 835 cm^{-1}, which has been ascribed to the bond-stretching (ν_3) vibrational mode. From the frequency ratio[4] of the ^{16}O and ^{18}O one can derive that oxygen is coupled to a residual mass of 58.9 amu, which suggests that indeed the two nearest silicon neighbors participate symmetrically in the oscillation. By solving the one-dimensional Schrödinger equation for the above reduced mass in this potential, we obtained 899 cm^{-1} for the ν_3 mode. As a rule SCF overestimates vibrational frequencies by 10%, so our result confirms the ν_3 assignment. The other modes are at

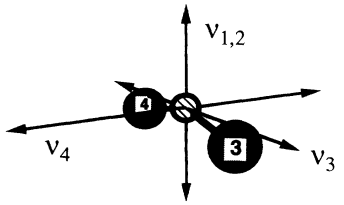

FIG. 3. The vibrational modes of substitutional oxygen in silicon.

lower frequencies; e.g., for the ν_4 mode we found the much lower wave number of 364 cm^{-1}.

F. Defect reorientation

An energy barrier of 0.38 eV was observed[1] for defect reorientation in the neutral charge state. We determined the saddle-point geometry in the closed shell approximation, which should give a good estimate. We find the saddle points very close to the $[\frac{1}{2}\frac{1}{2}\frac{1}{2}]$ positions, with the three silicon neighbors moved in by 0.17 Å along the new bond directions. From the closed shell energy difference in the two geometries, we estimate a barrier height of 0.25–0.35 eV, which is in reasonable agreement with experiment.

G. The positive charge state

Excitation ESE (Ref. 3) experiments situate the 0/+ level in the band gap at 0.76 eV below the conduction-band edge. No direct observations of $(V\text{-O})^+$ have been reported, however, although this charge state should be paramagnetic if it occurs. On the basis of modified neglect of differential overlap (MNDO) calculations, an oxygen displacement along the $[\bar{1}\bar{1}\bar{1}]$ direction was predicted.[13] This can be viewed as a change from divalent to trivalent behavior of oxygen. Such a change of valence also occurs when orthorhombic H_2O is converted into trigonal H_3O^+. Completely analogous cases are the NH_3 molecule and substitutional nitrogen in silicon and diamond.

We calculated the total energy of $[OSi_4H_{12}]^+$ for oxygen off-center displacements along the [111] and [001] directions, with the positions of the other cluster atoms frozen. The results are displayed in Fig. 4. An energy minimum of −0.8 eV with respect to the T_d position is observed for a displacement of 0.6 Å along the $[\bar{1}\bar{1}\bar{1}]$ direction. Silicon ligand relaxation lowers the minimum by an additional 0.3 eV. The on-axis dangling-bond ligand moves outward over a distance of 0.1 Å, while the off-axis ligands move inward by 0.1 Å along [311] directions. We have found a C_{2v} saddle point for an oxygen displacement of 0.5 Å along [001] at an energy of 0.3 eV below that of the T_d geometry. If the silicon ligands are allowed to relax as well, an additional energy lowering of 0.3 eV occurs. The final oxygen position is at 0.6 Å. The silicon ligands relax inward by 0.1 Å along the [110] direction, while the dangling-bond neighbors acquire a small outward relaxation of 0.04 Å. By this we have established that the positive charge state indeed has C_{3v} symmetry, with an estimated barrier against reorientation of about 0.5 eV. The unpaired electron preferentially occupies the dangling bond located at the on-axis ligand atom.

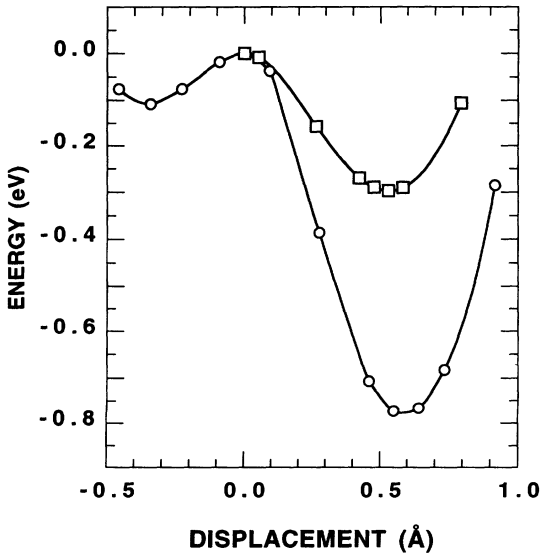

FIG. 4. Total energy of $[OSi_4H_{12}]^+$ vs oxygen displacement along z. ○: C_{2v} (00z); ●: C_{3v} (zzz).

IV. COMPARISON TO OTHER STUDIES

We found that the origin of the C_{2v} symmetry lowering is the chemical binding of divalent oxygen to the vacancy. This is already clear from the magnitude of the oxygen displacement and the energy gain involved, but even more so from the accompanying electronic restructuring of the center. The pseudo-JT mechanism[30,31] which states that symmetry lowering results from vibronic admixture of a low-lying orbitally degenerate excited state to the ground state, understates the role of such purely electronic effects.

Early calculations have been reviewed by DeLeo, Fowler, and Watkins,[13] who report an off-center displacement of 1.0 Å, close to our value. However, the off-center behavior was found to be completely quenched by a large inward ligand displacement of 0.35 Å in this MNDO study. From a calculation on the MO singlet, we find an inward T_d breathing relaxation of 0.1 Å with an energy gain of 0.4 eV. The value of this gain is comparable to the 0.6 eV gained from C_{2v} symmetry lowering that we obtained for this wave function. It is therefore likely that the quenching of the symmetry lowering results from the neglect of electron correlation in this calculation. Canuto and Fazzio[32] report an off-center displacement of 1.1 Å for $(V\text{-O})^0$ and an energy gain of 2.8 eV with respect to the T_d position. The value of the displacement is not far from ours, but the incomplete neglect of different overlap—based configuration interaction (CI) approach considerably overestimates the energy gained from the symmetry lowering. Silicon ligand relaxation was not considered in this calculation.

V. SUMMARY AND CONCLUSIONS

We have found that for $(V\text{-O})^0$ an oxygen off-center displacement of 0.95 Å occurs along the [001] direction. We conclude, from the electronic restructuring of the defect and from the magnitude of the displacements and energy gains involved, that the C_{2v} symmetry lowering is a chemical bonding effect. In a simple picture divalent oxygen bonds to the tetravalent vacancy, thereby saturating two of the four vacancy dangling bonds. We have found that the two oxygen-bonded silicon ligands move inward along the [110] direction by 0.19 Å with an energy gain of

the order of 1 eV. The dangling-bond ligands are predicted to stay very close to the perfect lattice positions, as was previously found by for the neutral vacancy in silicon.[25] Upon excitation to the triplet state $(V\text{-}O)^0$ shows geometry changes of the order of only a few pm with energy changes of the order of a meV. These numbers are consistent with the magnitude of distortions and energies we reported[25] for $Si:V^0$, a defect with similar weak covalent bonds. We have obtained an estimate for the singlet-triplet splitting of 0.16 eV. An experimental value is not available as yet. We have shown that the metastable triplet state decays nonradiatively through combined action of spin-orbit and vibronic couplings. Furthermore, we confirm theoretically that the observed infrared-absorption band at 835 cm^{-1} indeed results from the ν_3 asymmetric stretch mode. For the reorientational barrier we have obtained 0.25–0.35 eV, in reasonable agreement with experiment. We have obtained satisfactory agreement with experiment for the hyperfine interactions as well, and we have established that the agreement improves with increasing cluster size. We have established C_{3v} symmetry for the positive charge state. Our overall conclusion is that the quantum chemical hydrogen-terminated approach gives a complete and reliable description of substitutional oxygen in silicon.

ACKNOWLEDGMENTS

We thank Dr. R. Broer (University of Groningen), Dr. B. Th. Thole (University of Groningen), and Dr. M. C. van Hemert (University of Leiden) for support. This research forms part of the research program of the Netherlands Foundation of Fundamental Research on Matter (FOM), financially supported by the Netherlands Organization for Scientific Research (NWO). This research was sponsored by the Netherlands National Computer Facilities Foundation (NCF) for the use of supercomputer facilities, with financial support from the Netherlands Organization for Scientific Research (NWO).

*Author to whom all correspondence should be addressed. Electronic address: oos@ifm.liu.se

[1]G. D. Watkins and J. W. Corbett, Phys. Rev. **121**, 1001 (1961).
[2]A. M. Frens, J. Schmidt, W. M. Chen, and B. Monemar, Mater. Sci. Forum **83-87**, 357 (1992).
[3]A. M. Frens, M. E. Braat, A. B. Van Oosten, and J. Schmidt, Mater. Sci. Forum **117-118**, 195 (1993).
[4]J. W. Corbett, G. D. Watkins, R. M. Chrenko, and R. S. McDonald, Phys. Rev. **121**, 1015 (1961).
[5]K. L. Brower, Phys. Rev. B **4**, 1968 (1971).
[6]K. L. Brower, Phys. Rev. B **5**, 4274 (1972).
[7]W. M. Chen, B. Monemar, E. Janzén, and J. L. Lindström, Phys. Rev. Lett. **67**, 1914 (1991).
[8]A. B. Van Oosten (unpublished).
[9]K. L. Brower, Phys. Rev. Lett. **44**, 1627 (1980).
[10]K. L. Brower, Phys. Rev. B **26**, 6040 (1982).
[11]W. V. Smith, P. P. Sorokin, I. L. Gelles, and G. J. Lasker, Phys. Rev. **115**, 1546 (1957).
[12]Y. Ma, P. Skytt, N. Wassdahl, P. Glans, D. C. Mancini, J. Guo, and J. Nordgren, Phys. Rev. Lett. **71**, 3725 (1993).
[13]G. G. DeLeo, W. B. Fowler, and G. D. Watkins, Phys. Rev. B **29**, 3193 (1984).
[14]R. Broer, G. Aissing, and W. C. Nieuwpoort, Int. J. Quantum Chem. Quantum Chem. Symp. **22**, 297 (1988).
[15]A. Fazzio, C. R. Martins Da Cunha, and S. Canuto, Mater. Sci. Forum **83-87**, 463 (1992).
[16]P. A. Schultz and R. P. Messmer, Phys. Rev. B **34**, 2532 (1986).
[17]G. T. Surrat and William A. Goddard III, Phys. Rev. B **18**, 2831 (1978).
[18]I. Ortega-Blake, J. Tagüeña-Martínez, R. A. Barrio, E. Martínez, and F. Yndurain, Solid State Commun. **71**, 107 (1989).
[19]H. Dunning and P. J. Hay, in *Modern Theoretical Chemistry* (Plenum, New York, 1977), Vol. 3.
[20]S. Huzinaga (unpublished).
[21]W. J. Hunt, P. J. Hay, and W. A. Goddard III, J. Chem. Phys. **57**, 738 (1972).
[22]S. Fraga, J. Karwowski, and K. M. S. Saxena, *Handbook of Atomic Data* (Elsevier, Amsterdam, 1976).
[23]J. R. Morton and K. F. Preston, J. Magn. Res. **30**, 577 (1978).
[24]W. M. Chen, O. O. Awadelkarim, B. Monemar, J. L. Lindström, and G. S. Oehrlein, Phys. Rev. Lett. **64**, 3042 (1990).
[25]A. B. Van Oosten, A. M. Frens, and J. Schmidt, Mater. Sci. Forum **117-118**, 87 (1993).
[26]W. S. Veeman and J. H. Van Der Waals, Mol. Phys. **18**, 63 (1970).
[27]G. W. Robinson and R. P. Frosch, J. Chem. Phys. **38**, 1187 (1963).
[28]A. M. Frens, Ph. D. thesis, University of Leyden, 1993.
[29]D. R. Bosomworth, W. Hayes, A. R. L. Spray, and G. D. Watkins, Proc. R. Soc. London Ser. A **317**, 133 (1970).
[30]M. Lannoo, Phys. Rev. B **25**, 2987 (1982).
[31]F. G. Anderson, Phys. Rev. B **39**, 5392 (1989).
[32]S. Canuto and A. Fazzio, Phys. Rev. B **33**, 4432 (1986).
[33]J. S. M. Harvey, Proc. R. Soc. London Ser. A **285**, 581 (1965).

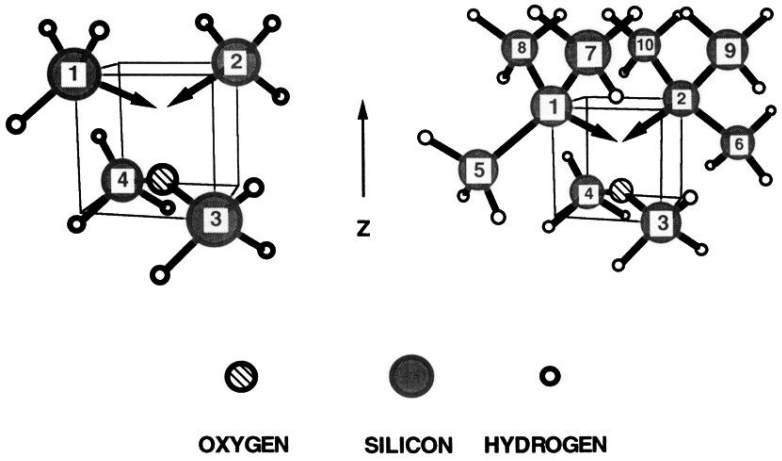

FIG. 1. The cluster models OSi_4H_{12} and $OSi_{10}H_{24}$.

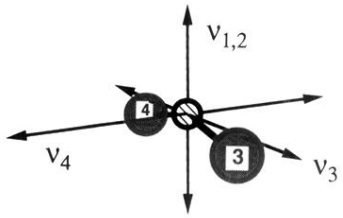

FIG. 3. The vibrational modes of substitutional oxygen in silicon.